Astron. Astrophys. 350, 945–954 (1999)

ASTRONOMY AND ASTROPHYSICS

Infrared spectra of carbon stars observed by the ISO SWS⋆

II. HCN and C_2H_2 bands at 14 μm

W. Aoki[1,2], **T. Tsuji**[3], **and K. Ohnaka**[3,4]

[1] Department of Astronomy, School of Science, The University of Tokyo, Bunkyo-ku, 113-0033 Tokyo, Japan
[2] National Astronomical Observatory of Japan, Osawa, Mitaka, 181-8588 Tokyo, Japan
[3] Institute of Astronomy, The University of Tokyo, Osawa, Mitaka, 181-8588 Tokyo, Japan
[4] Technische Universität Berlin, Institut für Astronomie und Astrophysik, Hardenbergstrasse 36, 10623 Berlin, Germany

Received 3 May 1999 / Accepted 5 August 1999

Abstract. We analyzed the mid-infrared spectra of 4 optical carbon stars and 4 candidates of infrared carbon stars obtained with the ISO SWS. It has been revealed that special care should be taken in determining the continuum levels for the analysis of the emission and absorption bands of HCN and C_2H_2 at 14 μm; otherwise the SiC emission at 11 μm as well as molecular absorption at 7.5 μm may lead to the misidentification of spectral features.

In the spectra of the two optical carbon stars TX Psc and V CrB, we detected the emission of the HCN $2\nu_2^0$–ν_2^1 band, which is direct evidence for the existence of HCN in their circumstellar envelopes. The excitation is almost due to radiative pumping, i.e. HCN molecules in the ground level are pumped to the $2\nu_2^0$ level by 7 μm photon from the photosphere or from the inner envelope. Since this emission band was detected in the spectrum of an Lb variable (TX Psc), a Mira variable (V CrB) and an infrared carbon star (IRC+10216, Cernicharo 1998), it is quite common in carbon stars over a wide range of the optical thickness of circumstellar envelopes.

On the other hand, the absorption features due to the C_2H_2 ν_5 bands at 13.7 μm were detected in all of the sources except for TX Psc. The absorption features turned out to be quite broad in the spectra of optical carbon stars. This broad absorption is attributed not only to the *Q* branches at 13.7 μm but also to the *P* and *R* branches between 12 and 16 μm. These features in the optical carbon stars are basically explained by the absorption in the photosphere or in the warm envelope close to the star. The detection of the C_2H_2 absorption in our infrared sources definitely confirms the carbon-rich nature of these objects. These absorption features would be formed in the inner envelope where the mid-infrared radiation originates.

Send offprint requests to: W. Aoki (aoki.wako@nao.ac.jp)

⋆ Based on observations with ISO, an ESA project with instruments funded by ESA Member States (especially the PI countries: France, Germany, the Netherlands and the United Kingdom) with the participation of ISAS and NASA.

Key words: stars: AGB and post-AGB – stars: atmospheres – stars: carbon – stars: circumstellar matter – stars: late-type – infrared: stars

1. Introduction

When low- and intermediate-mass stars evolve to red giants, especially to asymptotic giant branch (AGB) stars, the chemical composition in the stellar surface significantly changes. The most drastic change may be recognized in the formation of carbon stars. Another important characteristic in the AGB phase is the heavy mass loss which causes the growth of a circumstellar envelope. A variety of molecules are formed in the envelope, and the chemistry including carbon-bearing molecules in the envelope of carbon stars is an important subject in the study of the late stages of the stellar evolution.

For the study of the circumstellar envelopes of cool evolved stars, infrared molecular spectra have been investigated. However, the wavelength regions and objects observed were quite limited before the Infrared Space Observatory (ISO). The entire spectra from 2.5 to 45 μm became available for the first time thanks to the Short Wavelength Spectrometer (SWS) on board the ISO. The spectra obtained with the SWS have contributed to the study of molecular features originating in the circumstellar envelopes of cool stars as well as in the photospheres. For instance, the absorption and emission features of H_2O and CO_2 were discovered in oxygen-rich giants, and the existence of warm molecular envelopes in these sources was revealed (e.g. Tsuji et al. 1997, Justtanont et al. 1998, Ryde et al. 1999).

In this series of papers, we have been investigating the infrared spectra of carbon stars observed with the ISO SWS. The spectra up to 8 μm of 6 optical carbon stars were studied in our previous work (Aoki et al. 1998b, hereafter Paper I), where we identified a variety of features of diatomic molecules (CO, CS, CH and SiS) and of HCN. In that work, the dependence of the molecular features on C/O ratio was clearly shown, and most features can at least qualitatively be explained by our model photospheres. However, the absorption bands of CO and CS,

Table 1. Observations

star	spectral type	S_{25}/S_{12} [3]	AOT	obs. date
TX Psc	N, (C7,2)[1], Lb	−0.93	SWS06	26 Nov 1996
T Lyr	J, (C6,5)[1], Lb	−0.79	SWS06	12 Nov 1996
SS Vir	N, Mira	−0.82	SWS01,06	14 Jun 1996
V CrB	N,(CH?), (C6,2e)[1], Mira	−0.83	SWS06	29 Jul 1996
AFGL341	(C-rich)[2]	−0.35	SWS01	24 Jan 1998
AFGL2477	(C-rich)[2]	−0.16	SWS01	30 May 1997
IRAS 19454+2920	(C-rich)[2]	+0.40	SWS01	25 Apr 1997
IRAS 23321+6545	(C-rich)[2]	+0.48	SWS01	28 Jul 1996

[1] Yamashita (1972)
[2] Omont et al. (1993) suggested that they are carbon-rich based on the HCN emission in the radio range
[3] $S_{25}/S_{12} = \log(12F_{25\mu}/25F_{12\mu})$

especially their band head features, cannot be reproduced by our synthetic spectra. As a possible explanation of these features, we suggested the contribution of molecular emission in the outer atmosphere (the inner part of the circumstellar envelope) to the infrared spectra.

To investigate molecules in the circumstellar envelope, the spectra of the longer wavelength region are expected to be useful, since the photospheric radiation, which has its peak around 1–2 μm, decreases with the increase of wavelength. While few diatomic molecules have vibration-rotation bands in the wavelength region longer than 10 μm, there are strong bands of HCN (ν_2) and C_2H_2 (ν_5) in the 14 μm region. Since these polyatomic molecules are predicted to be abundant in a cool and carbon-rich environment, the observational investigation of these molecules is indispensable in the study of the chemistry in the circumstellar envelope.

The 14 μm region is hardly accessible by ground-based observations. However, for the bright infrared carbon star IRC+10216, the shorter wavelength part of the HCN ν_2 and the C_2H_2 ν_5 bands around 12 μm has been observed using the Fourier Transform Spectrometer (FTS), and the abundances of these molecules in the circumstellar envelope have been determined (e.g. Wiedemann et al. 1991, Keady & Ridgway 1993). These bands have also been studied using the SWS spectra. Yamamura et al. (1999) reported the detection of the C_2H_2 ν_5 bands in 11 objects and attempted to determine the column density of C_2H_2 in the circumstellar envelopes. The detection of HCN emission as well as C_2H_2 absorption in the 14 μm region in IRC+10216 was reported by Cernicharo (1998). These works show that more systematic studies of these bands for various types of carbon stars are required.

In this paper, we report the molecular features identified in the spectra of 8 sources obtained with the ISO SWS. In Sect. 2, we describe the observation and the data reduction. The molecular data used to produce the line list are summarized in Sect. 3. In Sect. 4, we first discuss the determination of the continuum level around 14 μm. After normalizing the spectrum, we show the identification of molecular features in each spectrum. In Sect. 5, we discuss the emission of HCN and the absorption of C_2H_2 in the circumstellar envelopes of carbon stars.

2. Observation and data reduction

Our observing program with the ISO SWS was presented in Paper I. The sample discussed in this paper is given in Table 1 with the spectral type and the details of the observation. The sample consists of 4 optical carbon stars including Mira variables and 4 infrared stars. TX Psc and T Lyr are Lb variables and have no heavy infrared excess up to 27 μm. The Mira variables SS Vir and V CrB show moderate infrared excess and strong emission at 11 μm which is usually attributed to SiC grains. The infrared sources have their peaks of radiation between 10 and 40 μm. Omont et al. (1993) suggested that they are carbon-rich based on the detection of the HCN emission in the radio range. While AFGL341 and AFGL2477 are in the region III of the IRAS color-color diagram defined by van der Veen & Habing (1988) and would be the AGB stars with thick circumstellar envelopes, IRAS 19454+2920 and IRAS 23321+6545 are in the region V and would be post-AGB objects with detached envelopes (Omont et al. 1993). Unfortunately, most of the carbon stars analyzed in Paper I for the 3–8 μm region are so faint at 14 μm that we could not investigate the molecular features, with TX Psc the only exception.

The resolution of the SWS06 spectra is about 1500 while that of SWS01 (speed1) spectra is about 200 at 14 μm. The composition of our sample is similar to that of Yamamura et al. (1999), though the objects are not identical at all. However, our sample includes the high resolution SWS06 spectra of optical carbon stars. Another SWS spectrum of TX Psc was analyzed by Jørgensen et al. (1999). They pointed out the time variation of the spectral features, comparing their observation with ours.

The data reduction was done with the SWS Interactive Analysis software (SWS IA) as in Paper I. One problem here is that the spectra of the 12–16 μm region are severely affected by the fringes due to the regular interference patterns, which depend on the exact pointing of the satellite at the time of the observation. To reduce this effect, we applied the defringing algorithm in the SWS IA package 'resp_inter' which tries to cancel the fringes by the small shift of the Relative Spectral Response Function (RSRF) in wavelength. However, such a procedure is somewhat questionable because the real features occurring at frequencies

close to the fringe pattern may be taken away. To check this effect, we show in Fig. 1 a comparison between the RSRF and the SWS06 spectra of two stars which were reduced with and without the defringing processes. Though the effect of the fringes is not significant in both spectra, we need special care in the discussion on the spectra processed with the defringing procedure. We note that some features at 12.4 μm in the observed spectra are probably due to the problem of the RSRF.

Another problem is that there are some discrepancies in flux between different AOT bands in the SWS spectra due to the uncertainty of the flux calibration. Though the absolute flux levels are not discussed in this paper, the discrepancies of the observed flux at 12 μm and at 16 μm can cause errors in the determination of the continuum levels for the optical carbon stars and the infrared stars, respectively (see Sect. 4.1). The flux levels were corrected by scaling with respect to the band 3A (12–16 μm). The slope of the spectrum in each AOT band was not changed after the reduction by the SWS IA. The flux discrepancies are at most 10%, except for the spectrum of SS Vir in which the discrepancy at 12 μm is about 25%.

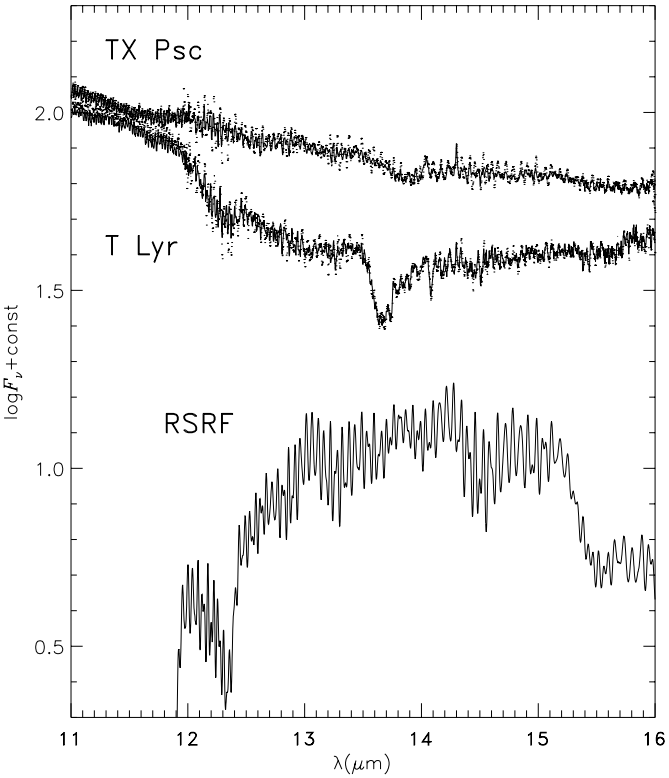

Fig. 1. The spectra of TX Psc and T Lyr reduced with and without the defringing processes (solid lines and dotted lines, respectively). The bottom is the Relative Spectral Response Function (RSRF)

3. Molecular data

In the 14 μm region, the HCN ν_2 bands and the C_2H_2 ν_5 bands can be found, both of which are perpendicular bands and have the strong *Q* branches (Herzberg 1945).

The molecular data of HCN used to produce the line list of the ν_2 bands were given in Paper I. We calculated the energy levels for $v_2 \leq 4$ and $v_3 \leq 1$, which cover up to about 3000 cm^{-1}.

C_2H_2 is characterized by the two degenerate vibrations, and the quantum number for the total vibrational angular momentum k ($= l_4 + l_5$) should be considered. A full Hamiltonian representing bending energy levels up to $v_4 + v_5 \leq 4$ was presented by Herman et al. (1991). We calculate the energy levels using their Hamiltonian and the molecular constants determined by Kabbadj et al. (1991). For the calculation of line intensities, we used the transition dipoles, Herman-Wallis factors, and Hönl-London factors derived by Weber et al. (1994). However, the Herman-Wallis factors derived by Weber et al. (1994) are not enough to calculate the line intensities for high excitation bands. Therefore, the correction by these factors was neglected for high excitation bands.

4. Identification of molecular features

In this section, we first discuss the determination of the continuum level around 14 μm. After normalizing the spectrum, we identify the molecular emission and/or absorption in each spectrum.

4.1. Spectral features in 7–15μm

The continuum levels around 14 μm should carefully be determined for optical carbon stars, because the emission of SiC at 11μm may affect the spectral features of this wavelength region. Furthermore, the 8–11 μm feature should be discriminated from the absorption in 7–8 μm due to HCN, C_2H_2 and CS. The identification of these features is another important subject which has been studied based on low resolution spectra (see below).

In Fig. 2, we show the spectra of the optical carbon stars in our sample between 7 and 20 μm, which are rebinned to a resolution of 50. Since TX Psc and T Lyr have no strong infrared excess, we fitted with the 3000 K Planck function which roughly represents the photospheric component. As can be seen in Fig. 2, there is no emission feature at 11 μm in the spectrum of TX Psc, while there is broad absorption around 14 μm which can be attributed to HCN (Sect. 4.2), and the absorption of the CS fundamental bands at 7.5 μm (Paper I). The 7–12 μm region of the spectrum of T Lyr can be interpreted as due to the absorption of the C_2H_2 $\nu_4 + \nu_5$ bands in 7–8 μm and due to the weak emission of SiC around 11 μm. There is a small uncertainty ($\leq$0.05 dex) in the fitting, but we undoubtedly found a broad absorption feature from 12 to 16 μm which can be attributed to the *P* and *R* branches of the C_2H_2 ν_5 bands, in addition to the strong *Q* branches at 13.7 μm (see Sect. 4.3).

On the other hand, the spectra of the Mira variables SS Vir and V CrB are strongly affected by the emission from dust shells, and can no longer be fitted with the 3000 K Planck function. To estimate the continuum levels, we try to fit a 1300 K Planck function to the observed spectra of these stars (Fig. 2). While there is strong 11 μm emission of SiC, broad absorption bands

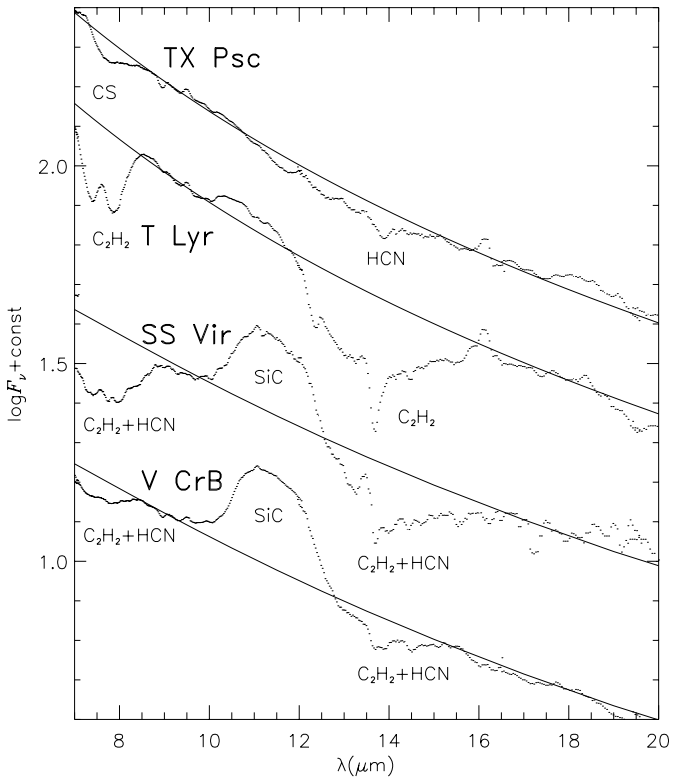

Fig. 2. The spectra of optical carbon stars (dots). The resolution is reduced to 50. The molecular features of CS, HCN and C_2H_2 as well as the SiC emission are identified. The solid lines fitted to the spectra of TX Psc and T Lyr are the 3000 K Planck function, while those fitted to the spectra of SS Vir and V CrB are the 1300 K one. These lines fitted to the spectra are used as the continuum levels around 14 μm

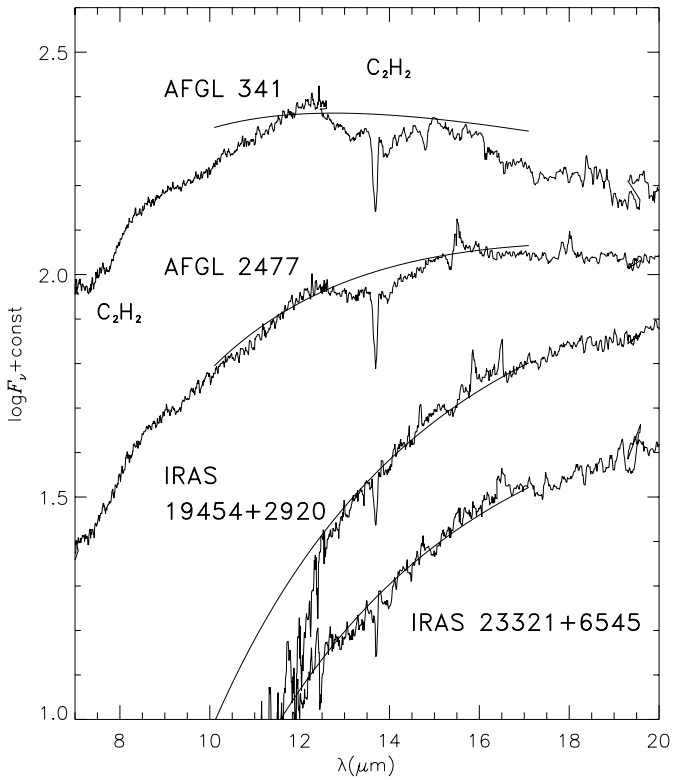

Fig. 3. The spectra of infrared stars and the fit with the Planck functions. The temperatures of the Planck functions are 400 K, 270 K and 170 K for AFGL341, AFGL2477 and the other two stars, respectively. The absorption of C_2H_2 at 13.7 μm is identified in every spectrum

around 7 μm and 14 μm are recognized in these spectra. These absorption bands are attributed to HCN and C_2H_2 (Sect. 4.4).

As shown above, the determination of the continuum levels relates to the understanding of the 8–11 μm features. The emission features in this wavelength region were studied by Sloan et al. (1998) based on the IRAS Low Resolution Spectra (LRS) for 96 carbon stars. They classified TX Psc and V CrB into the classes 'N' (no feature) and 'SiC' (11.2 μm emission), respectively, and these results were confirmed by our SWS spectra. However, our analysis of the spectrum of T Lyr does not support their classification of this star into the 'SiC ++' class (11 μm and 8.5–9.0 μm emission features), but suggests that the apparent emission feature at 8.5–9 μm is due to the strong absorption of the C_2H_2 $\nu_4 + \nu_5$ bands at 7.5 μm, as Sloan et al. (1998) pointed out as another interpretation. They commented the two characteristics of the SiC++ sources. The one is that all but one of the six SiC++ sources are SRb or Lb variables. The other is that the C/O ratios of the stars in this class are significantly higher than in other classes (e.g. SiC class) according to Lambert et al. (1986). They suggested a correlation between the C/O ratio and the 8.5–9.0 μm emission. However, the higher C/O ratio can cause the stronger C_2H_2 absorption at 7.5 μm in the spectra of SRb and Lb variables, while the absorption may be diluted by the dust emission in Mira variables even if the photospheric C_2H_2 absorption is strong due to the high C/O ratio. Hence, we suggest that the SiC++ sources should be interpreted as the SiC stars with strong C_2H_2 absorption at 7.5 μm. Further, the spectrum of SS Vir, which was classified into the 'Broad 1' class (11 μm emission with short-wavelength excess) by Sloan et al. (1998), can also be explained by the 7.5 μm absorption, the 11 μm emission and the 14 μm absorption. We note, however, that more careful investigations of the spectra in this class are required, given the large uncertainty in the flux calibration of our SWS spectrum of SS Vir.

The observed spectra of our infrared sources are shown in Fig. 3. The 13.7 μm absorption bands which are attributed to the *Q* branches of the C_2H_2 ν_5 bands (Sect. 4.5) were clearly detected in every spectrum. In the spectra of AFGL341 and AFGL2477, the absorption features which can also be attributed to C_2H_2 are recognized in the 7–8 μm region. The spectra of IRAS 19454+2920 and IRAS 23321+6545 in the wavelength shorter than 12 μm are quite noisy. This fact is consistent with the characteristics of post-AGB objects with detached envelopes (see Sect. 4.5). As shown in Fig. 3, we fitted the Plank functions with 170–400 K for the 10–17 μm region and regarded them as continuum levels. In the spectra of AFGL341 and AFGL2477, the broad absorption between 13 and 15 μm, which can be attributed to the *P* and *R* branches of the C_2H_2 ν_5 bands, was also identified in addition to the narrow absorption of the *Q* branches at 13.7 μm.

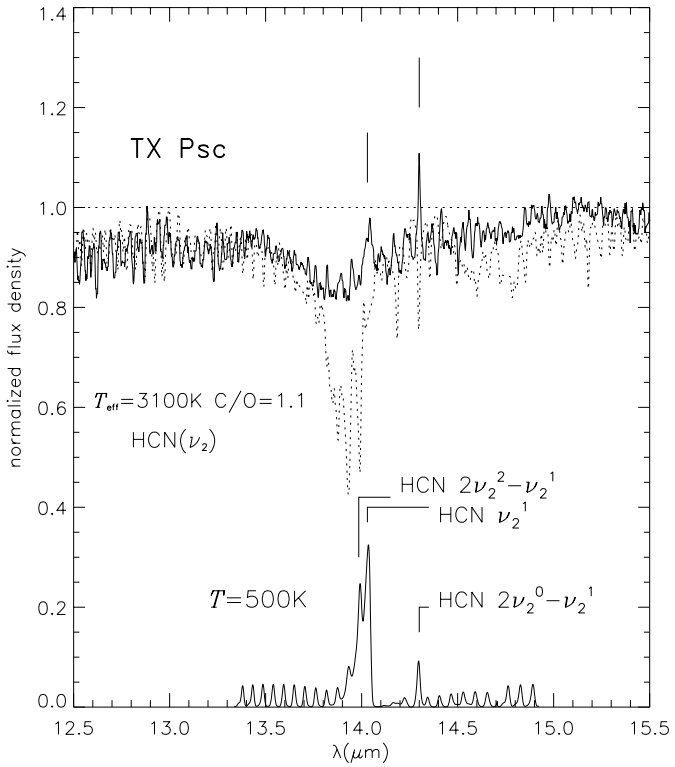

Fig. 4. The normalized spectrum of TX Psc (solid line) and a synthtic spectrum of the HCN ν_2 bands based on the model photospheres with $T_{\rm eff}$=3100 K and C/O=1.1 (dotted line). The bottom is the emission spectrum of the HCN bands predicted for T=500 K. The emission of the HCN $2\nu_2^0$–ν_2^1 and ν_2^1 bands is identified

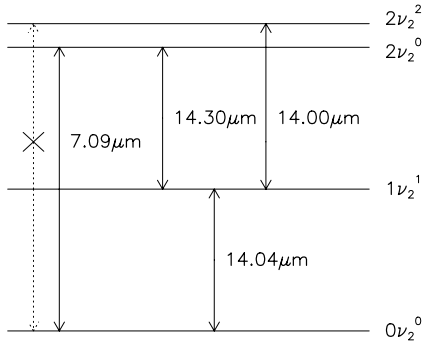

Fig. 5. The energy levels of HCN and the wavelengths of transitions in the ν_2 bands

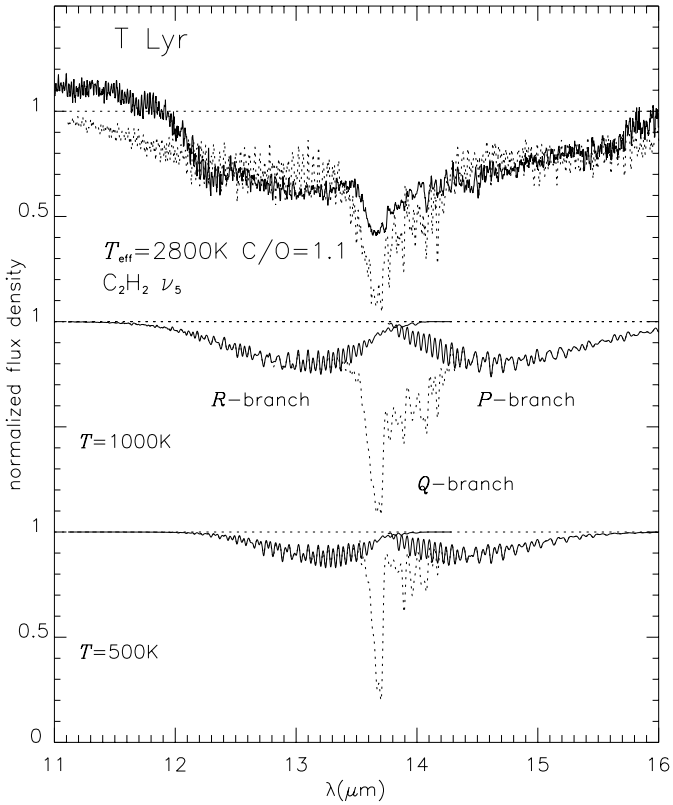

Fig. 6. The normalized spectrum of T Lyr (solid line) and a synthetic spectrum of the C_2H_2 ν_5 bands based on the model photospheres with $T_{\rm eff}$=2800 K and C/O=1.1 (dotted line). The middle and bottom are the absorption spectra of the C_2H_2 bands predicted for T=1000 K and 500 K, respectively. The *P* and *R* branches in the predicted spectra are shown by the solid lines, whereas the spectrum including *Q* branches is shown by the dotted line

4.2. TX Psc: HCN absorption and emission

The 14 μm region of the normalized spectrum of TX Psc is shown in Fig. 4. In this figure, the synthetic spectrum of the HCN ν_2 bands based on the model photosphere with $T_{\rm eff}$=3100 K and C/O=1.1 is also shown by the dotted line. The HCN absorption feature appears at 13.9 μm in the spectrum of TX Psc, but is much weaker than predicted, while the 3 μm HCN band is reasonably reproduced by the synthetic spectrum based on the same model photosphere (Paper I). The weakness of the absorption feature of HCN in the observed spectrum may indicate the HCN emission in the outer atmosphere as in the case of the CO and CS features discussed in Paper I.

In addition, the emission features of HCN at 14.04 and 14.30 μm were directly detected in the spectrum of TX Psc. In Fig. 4, the emission spectrum of the HCN ν_2 bands calculated assuming a temperature of 500 K is also shown. The emission features at 14.04 and 14.30 μm can be attributed to the *Q* branches of the HCN ν_2^1 and $2\nu_2^0$–ν_2^1 bands, respectively (see Fig. 5 where the energy levels of HCN and the wavelengths of the transitions are shown). The emission features in the SWS06 spectrum of TX Psc are unlikely due to the fringes or due to errors in the defringing process if we compare the spectrum with the RSRF (Fig. 1). We discuss the details of the HCN emission from the circumstellar envelope of TX Psc in Sect. 5.1.

4.3. T Lyr: C_2H_2 absorption

Fig. 6 shows the normalized spectrum of T Lyr (top) and the absorption profile of the C_2H_2 ν_5 bands for 1000 K and 500 K (middle and bottom, respectively). We can recognize the broad *P* and *R* branches of the C_2H_2 ν_5 bands between 12 and 16 μm, in addition to the strong *Q* branches at 13.7 μm. We note that the shorter wavelength region of the spectra is affected by the 11 μm emission as well as by the instrumental problem at 12.4 μm (see

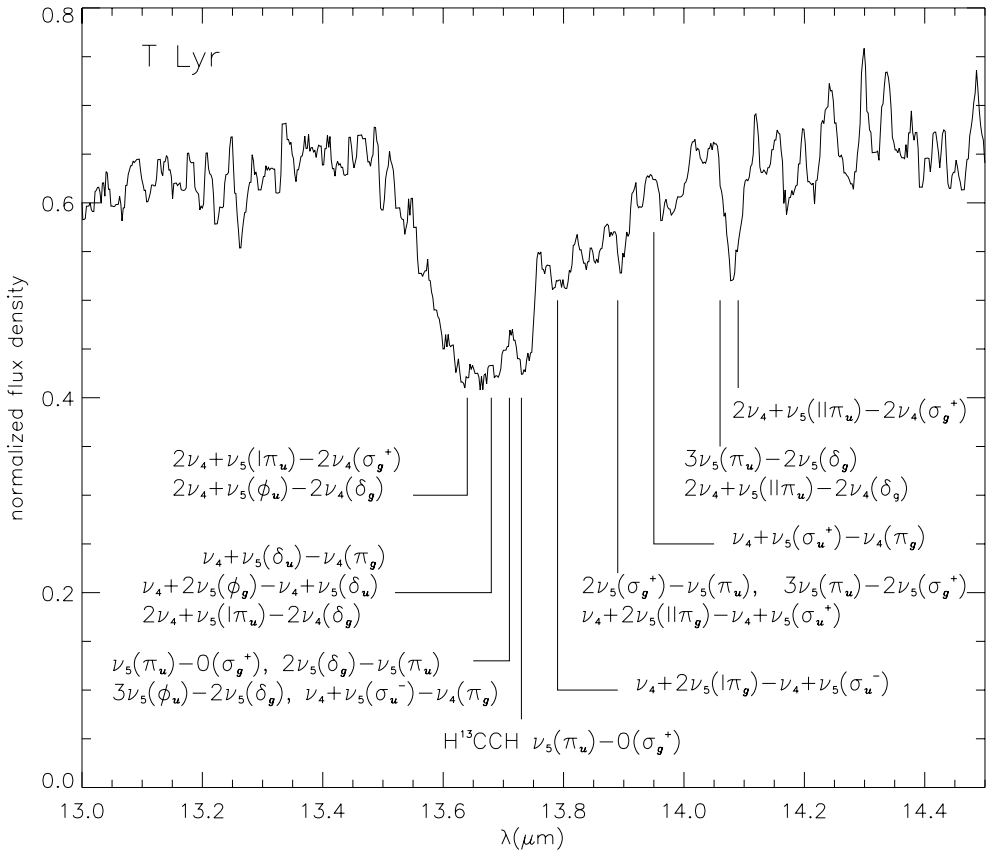

Fig. 7. The normalized spectrum of T Lyr with the identification of the *Q* branches of the C_2H_2 ν_5 bands, including that of the $H^{12}C^{13}CH$ ν_5^1 band

Sect. 2). A synthetic spectrum based on our model photosphere is also shown in Fig. 6 (the dotted line in top). Since the stellar parameters (e.g. $T_{\rm eff}$, C/O) were simply adopted so that the synthetic spectrum can reproduce the *P* and *R* branches of the observed spectrum, we do not insist on these values as the stellar parameters of T Lyr.

The temperature of the layers contributing to this absorption is estimated to be higher than 1000 K, because of the broad absorption feature. Since the temperature of the photosphere where C_2H_2 is abundant is 1000–1500 K in cool carbon stars, the broad absorption of C_2H_2 can be interpreted as of the photospheric origin. However, the synthetic spectra based on our model photospheres cannot reproduce the absorption feature. For instance, the *Q* branches in the observed spectrum are much weaker than those in the synthetic spectrum which reproduces the *P* and *R* branches (Fig. 6). One possible explanation of this weakness of the *Q* branches is the dilution of the absorption feature by dust emission, but that would not completely explain the weakness of the *Q* branches in the observed spectrum, since the infrared excess of this star is quite small.

The individual *Q* branches of the C_2H_2 ν_5 bands can be identified. The wavelength region around 13.7 μm is shown in Fig. 7 where the identification of the *Q* branches is given. In addition to the *Q* branches of $H^{12}C^{12}CH$, the ν_5^1 band of $H^{12}C^{13}CH$ at 13.73 μm was also detected. This result is quite reasonable, because T Lyr is a J-type star, i.e. ^{13}C-rich carbon star. While C_2H_2 bands were clearly identified, no evident HCN band was detected in the spectrum of T Lyr. This is consistent with the result of the analysis of the high resolution FTS spectrum around 3 μm by Ridgway et al. (1978). The deficiency of HCN in T Lyr would be due to the low nitrogen abundance (N/C=0.04 was derived by Lambert et al. 1986).

No high resolution and high quality spectrum of C_2H_2 in this wavelength region has been reported, except for the SWS06 spectrum of IRC+10216 by Cernicharo (1998) and by Yamamura et al. (1999). The spectrum of T Lyr can be a prototype of C_2H_2 absorption originating in the photosphere or in the warm envelope for optical carbon stars, while the spectrum of IRC+10216 is that for infrared carbon stars.

4.4. Mira variables: HCN and C_2H_2 absorption and HCN emission

The normalized spectra of SS Vir and V CrB are shown in Fig. 8. In the spectrum of SS Vir, the broad absorption of the C_2H_2 ν_5 bands was detected as in the case of T Lyr, despite the lower quality of the data and the rather uncertain normalization. In the spectrum of V CrB, the absorption feature at 13.9 μm which can be attributed to the HCN ν_2 bands was detected, in addition to the 13.7 μm absorption of C_2H_2. The broad absorption bands in the spectra of these Mira variables mean that the absorption originates in the photosphere or in the warm envelope close to the photosphere.

The absorption features in Mira variables are much weaker than those of T Lyr, and this would partly be explained by the stronger dust emission in these Mira variables which fills the

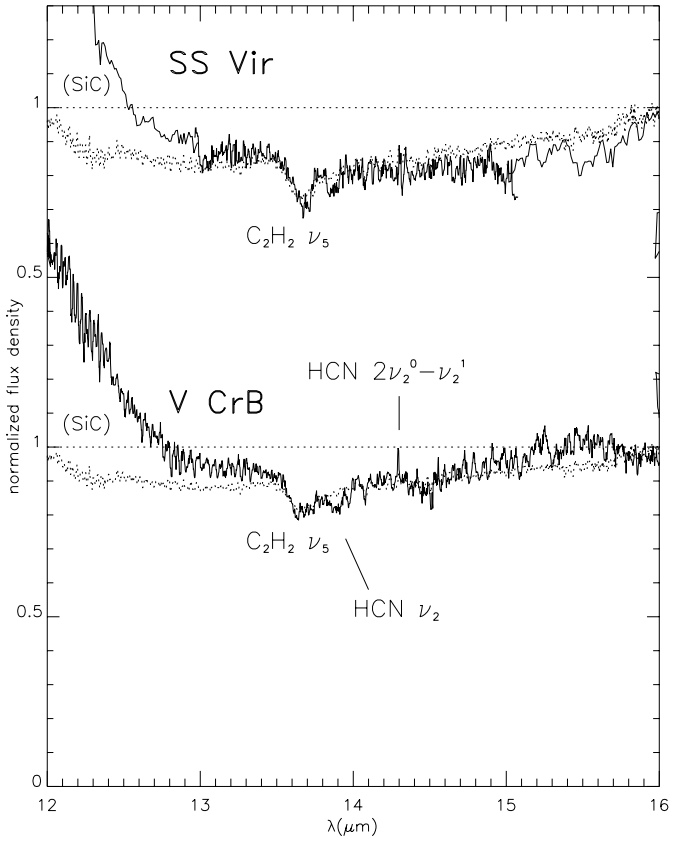

Fig. 8. The normalized spectra of two Mira variables. The absorption features of the C_2H_2 ν_5 bands are identified. In the spectrum of V CrB, the emission of the HCN $2\nu_2^0$–ν_2^1 band is detected as well as the absorption of the HCN ν_2 bands. The dotted lines are the templates representing the C_2H_2 absorption in the photosphere and dust emission in the envelope (see text)

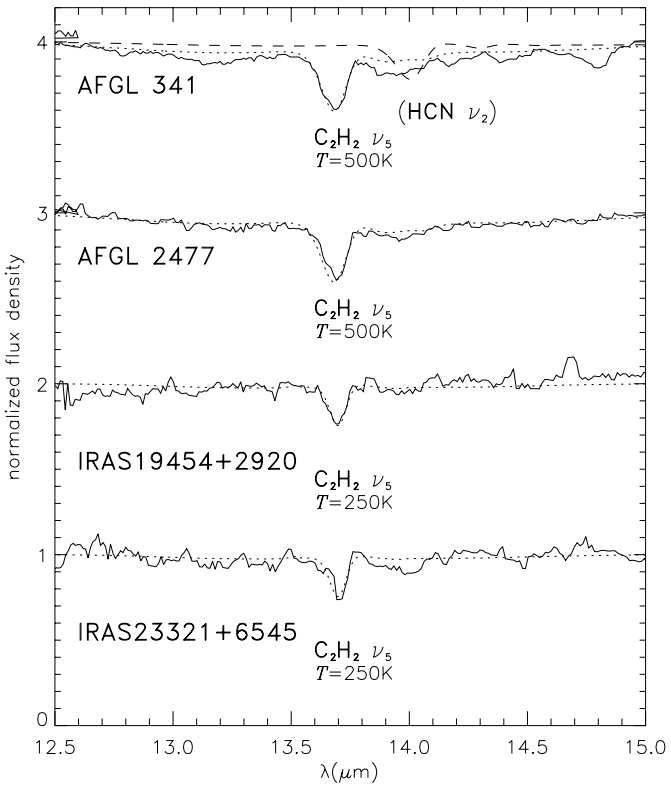

Fig. 9. The normalized spectra of infrared carbon stars (solid lines) and predicted spectra of the C_2H_2 ν_5 bands (dotted lines) and of the HCN ν_2 bands (dashed line)

molecular absorption. For a comparison, we tried to produce the template of the spectrum which represents the C_2H_2 absorption in the photosphere (and maybe in the warm envelope close to the star) and the dust emission in the envelope. We used the spectrum of T Lyr as the component of C_2H_2 absorption originating in the photosphere, since our model photospheres may not necessarily reproduce the photospheric absorption (see Sect. 4.3). To represent the contribution of dust emission, we added a constant to the flux density of the photospheric component, and normalized it again. The spectra obtained by this procedure are shown by the dotted lines in Fig. 8. The contribution by the dust emission is assumed 30% and 50% for SS Vir and V CrB, respectively. Except for the HCN features, the broad absorption bands are reasonably reproduced by these templates. Thus the C_2H_2 absorption features in these Mira variables can simply be explained by the absorption in the photosphere or in the warm envelope close to the star.

The photospheric spectra of Mira variables are recently studied based on the model atmospheres taking dynamics due to the stellar pulsation into consideration (e.g. Aringer et al. 1999). The absorption features may be weakened by the dynamical effect, but it is not easy to distinguish the effect from the dilution of the absorption by the dust emission. The quantitative analysis including dynamics in the atmosphere and dust emission in the circumstellar envelope should be done in future works.

The emission of the HCN $2\nu_2^0$–ν_1^1 band at 14.3 μm was identified in V CrB as in TX Psc. We discuss the HCN emission from the circumstellar envelope of carbon stars in Sect. 5.1.

4.5. Infrared carbon stars: C_2H_2 absorption

In Fig. 9, the normalized spectra of the 4 infrared stars are shown by the solid lines with the absorption profiles of C_2H_2 assuming 500 K or 250 K by the dotted lines. The *Q* branches of the C_2H_2 bands at 13.7 μm were clearly detected in every spectrum. Therefore, these sources have obviously carbon-rich envelopes. These objects were classified as carbon-rich stars by Omont et al. (1993) based on the detection of the HCN emission at 89 GHz. However, the HCN emission in the radio range may be somewhat questionable as a criterion to distinguish carbon stars from oxygen-rich stars, because the emission originates in the quite cool envelope far from the central star and has been sometimes detected even in the sources with OH masers. Our detection of C_2H_2 absorption finally confirms the carbon-rich nature of these infrared sources.

The absorption features of the *Q* branches in the spectra of AFGL341 and AFGL2477 are rather broad. Moreover, the *P* and *R* branches are also detected in these spectra. For these reasons,

the temperature of the layer which contributes to the absorption is roughly estimated to be 500 K. This indicates that the absorption originates in the warm inner envelope. Since the *P* and *R* branches are not clearly identified in IRAS 19454+2920 and IRAS 23321+6545 (see Figs. 3 and 9), the temperature of the layer contributing to the C_2H_2 absorption in these sources would be lower than in AFGL341 and AFGL2477, and estimated to be about 250 K. However, this temperature is still higher than that of the region where dust grains contribute to the peak of the flux around 30 μm ($\sim$ 100 K). These results mean that the radiation at 14 μm originates in the inner envelope, and the absorption features would be produced by the C_2H_2 coexisting with dust grains, while the peak of the flux around 30 μm originates in the cooler and more extended envelope. The result that the temperature of the shells where C_2H_2 absorption originates is lower in IRAS 19454+2920 and IRAS 23321+6545 than in AFGL341 and AFGL2477 is quite reasonable, because the warm envelopes are probably missing in these post-AGB objects.

Though HCN is also expected to be abundant in these stars, the HCN bands are not clearly identified in the spectra. This would be because the HCN bands are weaker than those of C_2H_2 due to the smaller oscillator strengths, even if the same abundance is assumed for HCN and C_2H_2. We show the predicted spectrum of the HCN ν_2 bands for the same column density as that of C_2H_2 by the dashed line with the spectrum of AFGL341 in Fig. 9. Higher resolution or higher quality spectra are required to derive the abundance ratio of HCN to C_2H_2.

5. Discussion

5.1. HCN emission from the circumstellar envelope

As shown in Sect. 4, the emission of the HCN $2\nu_2^0$–ν_2^1 band was detected in the spectra of TX Psc which has no strong dust emission and of V CrB which is a Mira variable with moderate infrared excess. The detection of this emission band was also reported by Cernicharo (1998) for the well-known infrared carbon star IRC+10216. Hence, this emission band is quite common in carbon stars over a wide range of the optical thickness of the circumstellar envelope, and can be a useful probe to investigate the structure of the envelope. We discuss here the emission of the *Q* branch of the $2\nu_2^0$–ν_2^1 band in the spectrum of TX Psc for which the basic physical parameters (e.g. stellar radius, mass loss rate) are known.

Since the HCN emission features originating in the envelope are blended with the absorption in the photosphere (and partly in the circumstellar envelope), the uncertainty of the measurement of the emission is unavoidable. However, the emission feature of the *Q* branch of the $2\nu_2^0$–ν_2^1 band at 14.30 μm is at least as strong as that of the ν_2^1 band at 14.04 μm. If the region where the emission of the $2\nu_2^0$–ν_2^1 band originates is dense enough to be in thermal equilibrium, the temperature should be quite high ($\sim$ 2000 K). However, the *Q* branch of the $2\nu_2^2$–ν_2^1 band which is expected at 14.00 μm is not seen in the spectrum of TX Psc. This means that the excitation to the $2\nu_2^0$ level is mainly due to radiative pumping by 7 μm photon, because the transition from the ground level to the $2\nu_2^2$ level is forbidden due to the selection rule on the quantum number l while the transition to the $2\nu_2^0$ is permitted. Then the temperature of the region where the emission features originate is not necessarily so high.

The probability of collisional excitation is estimated by $C \sim N_{\rm H_2}\sigma v$. The cross section, σ, is of the order of 10^{-15}cm^2, and the velocities of the molecules, v, for the relevant temperature are about 1 km s^{-1}. The Einstein coefficients of the transitions $2\nu_2^0$ and $2\nu_2^0$–ν_2^1 are 2.1 s^{-1} and 3.3 s^{-1}, respectively (Maki et al. 1995). Therefore the radiative processes dominate, if the density is lower than 10^{10} cm^{-3}. Since the densities of the outer atmosphere and the circumstellar envelope of TX Psc would not be so high except for the innermost layer (Aoki et al. 1998a), the above interpretation of the excitation mechanism of the HCN molecule is quite reasonable.

The flux of the *Q* branch of the $2\nu_2^0$–ν_2^1 band measured for TX Psc is about 2×10^{-12} erg s^{-1} cm^{-2}. The uncertainty would be as large as a factor of 2, because this emission band blends with the photospheric absorption. We now estimate the flux of the $2\nu_2^0$–ν_2^1 band expected from the circumstellar envelope of TX Psc, and compare it with the observed one. In the calculation, we assume the pure radiative processes, i.e. the HCN molecule in the ground level is pumped to the $2\nu_2^0$ level by 7 μm photon from the photosphere, and radiatively decays to the ν_2^1 or to the ground level. The fraction of the $2\nu_2^0$–ν_2^1 transition is $\alpha = A_{2\nu_2^0-\nu_2^1}/(A_{2\nu_2^0-\nu_2^1}+A_{2\nu_2^0}) \sim 0.6$. We also assume an optically thin circumstellar envelope with a constant mass loss rate ($\dot{M}$), a constant expansion velocity ($v_{\rm exp}$) and a constant abundance of HCN ($\epsilon_{\rm HCN}$).

The number of HCN molecules in the spherical shell with radius r and thickness dr is

$$dn_{\rm HCN} = 4\pi r^2 dr \cdot n\epsilon_{\rm HCN}. \quad (1)$$

The density n is given by $n = \dot{M}/(4\pi r^2 v_{\rm exp}\mu m_{\rm H})$, where μ is the mean molecular mass. The flux of the $2\nu_2^0$–ν_2^1 band from this shell is

$$F_{2\nu_2^0-\nu_2^1}(r)dr = \alpha\frac{1}{4\pi D^2}dn_{\rm HCN}\frac{D^2}{r^2}f_{\lambda_0}\sigma_{\lambda_0}\delta\lambda, \quad (2)$$

where D is the distance to the star, λ_0 is the wavelength of the $2\nu_2^0$ transition (7.09 μm), and f_{λ_0} is the 7 μm flux density observed (200Jy=1.2×10^{-4} erg s^{-1} cm^{-2} cm^{-1}). The cross section, σ_{λ_0}, is given by $(\pi e^2/m_{\rm e}c^2)(\lambda_0^2 f_{2\nu_2^0}/\delta\lambda)$, where $f_{2\nu_2^0}$ is the band oscillator strength of the $2\nu_2^0$ transition (1.6×10^{-6}), and $\delta\lambda$ is the width of lines in the $2\nu_2^0$ band. The stimulated emission is ignored here. The integrated flux expected to be observed is

$$\begin{aligned} F^{\rm int}_{2\nu_2^0-\nu_2^1} &= \int_{r_{\rm in}}^{\infty} F_{2\nu_2^0-\nu_2^1}(r)dr = \alpha\frac{e^2\lambda_0^2 f^0_{2\nu_2}}{4m_{\rm e}c^2\mu m_{\rm H}}f_{\lambda_0}\frac{\dot{M}\epsilon_{\rm HCN}}{v_{\rm exp}r_{\rm in}} \\ &\sim 6.6\times10^{-12}\left(\frac{\epsilon_{\rm HCN}}{6\times10^{-6}}\right)\left(\frac{r_{\rm in}}{R_\star}\right)^{-1}\left(\frac{\dot{M}}{10^{-7}M_\odot{\rm yr}^{-1}}\right) \\ &\quad\times\left(\frac{v_{\rm exp}}{10{\rm km\,s^{-1}}}\right)^{-1}{\rm erg\,s^{-1}cm^{-2}}, \end{aligned} \quad (3)$$

where $R_\star$ is the stellar radius ($200R_\odot$). The abundance of HCN in the circumstellar envelope has not yet been measured for

TX Psc, though the upper limit, 2.2×10^{-5}, was determined by Olofsson et al. (1993b) using the emission line in the radio range. We here adopt $\epsilon_{\rm HCN} = 6\times10^{-6}$ which was derived from the calculation of photodissociation and molecular abundance in the circumstellar envelope of TX Psc by Wirsich (1997). The expansion velocity of the circumstellar envelope is 10.5 km s^{-1} which was determined by Olofsson et al. (1993a) using the CO emission in the radio range. The order of the flux expected by the above discussion is 10^{-12} erg s^{-1} cm^{-2}, which is consistent with the observed one (2×10^{-12} erg s^{-1} cm^{-2}). This means that the emission of the HCN would be reasonably explained by the radiative processes in the circumstellar envelope.

For the more detailed discussion, the parameters, e.g. $v_{\rm exp}$, should be given as functions of radius from the central star. For instance, the velocity in the inner envelope would be much smaller than the terminal velocity, and the density of HCN in the inner envelope would be higher than that estimated in the above simple calculation. Further, in the innermost layer, the effect of the collisional transition may be important because of the higher density. Since the HCN emission is not expected from the dense region where collision dominates, the extent of the dense region can be derived as $r_{\rm in}$ in the above discussion. Thus, the HCN emission can be used as a constraint for the future modeling of the circumstellar envelope of carbon stars.

In oxygen-rich giants, the detection of the CO_2 emission (ν_2 bands) around 15 μm was reported by Justtanont et al. (1998) and Ryde et al. (1999). The 15 μm emission features were also detected in our M giants for which the CO_2 absorption at 4.2 μm was studied in Tsuji et al. (1997). These emission bands of CO_2 in the 13–16 μm region of oxygen-rich stars have not yet been consistently explained. For example, the ν_2^1 band at 15.0 μm which is expected to be the strongest is rather weaker than the ν_1–ν_2^1 band at 13.9 μm and the $2\nu_2^0$–ν_2^1 band at 16.2 μm. This behavior may be similar to that of the HCN 14 μm emission features discussed above. As a possible explanation of these CO_2 emission features, a two-layer model of the circumstellar envelope was proposed by Ryde et al. (1999). Similar interpretation may be possible for the HCN emission features in the 14 μm region in carbon stars. But the situation is more complicated because the photospheric contribution is large in the HCN features in carbon stars contrary to the CO_2 features in oxygen-rich stars.

5.2. C_2H_2 in the circumstellar envelope

To investigate the abundance distribution of C_2H_2 in the circumstellar envelope is an important subject, because this molecule may play a significant role in dust formation in carbon stars. The decrease of the C_2H_2 abundance by at least a factor of 5 from 100 to $1000R_*$ in IRC+10216 was shown by Keady & Hinkle (1988) based on the high resolution spectra of C_2H_2 and C_2H, and this result was attributed to the accretion of the molecule onto grains.

However, there is no evidence for the abundance variation of C_2H_2 in the circumstellar envelope of the optical carbon stars in our sample. While the existence of HCN in the circumstellar envelope was confirmed by the emission bands, no emission feature of C_2H_2 was detected in the spectra. If we assume a circumstellar envelope like that of TX Psc, some emission features of the *Q* branches of the C_2H_2 ν_5 bands, e.g. the $\nu_4+\nu_5(\sigma)$ – ν_4 bands, are expected around 13.7 μm. However, no distinct emission of C_2H_2 was detected even in the spectrum of T Lyr where the C_2H_2 absorption was clearly identified (Fig. 7). This may simply be due to the highly crowded absorption bands of C_2H_2 which mask the emission features. Higher resolution spectroscopy and/or more detailed analysis are required for this band which will bring useful information on chemistry in the circumstellar envelope.

Since the C_2H_2 absorption in the optical carbon stars is quite broad, and the infrared excesses are not large, the absorption of C_2H_2 would be due to the hot component, i.e. the absorption in the photosphere or in the warm inner envelope close to the star with $T \gtrsim 1000$ K. However, this does not necessarily imply the depletion of C_2H_2 by the accretion onto grains in the cool outer envelope of these stars. If we assume a constant mass loss rate ($\dot{M}$), a constant expansion velocity ($v_{\rm exp}$) and a constant C_2H_2 abundance ($\epsilon_{\rm C_2H_2}$), the column density of C_2H_2 from $r = r_{\rm in}$ to $r_{\rm out}$ is represented by

$$\begin{aligned} N_{\rm C_2H_2} &= \int_{r_{\rm in}}^{r_{\rm out}} \frac{\dot{M}}{4\pi r^2 v_{\rm exp}\mu m_{\rm H}}\epsilon_{\rm C_2H_2}\,dr \\ &= \frac{\dot{M}\epsilon_{\rm C_2H_2}}{4\pi v_{\rm exp}\mu m_{\rm H}}\frac{1}{r_{\rm in}}(1-\frac{r_{\rm in}}{r_{\rm out}}). \end{aligned} \quad (4)$$

For example, if the hot layer is defined as the region from stellar surface to $5R_*$, the column density of C_2H_2 in the hot layer ($r < 5R_*$) is higher by a factor of 4 than that in the cool layer ($r > 5R_*$). Since the density in the hot layer should be much higher due to the lower expansion velocity than in the cool outer layer, the column density in the hot layer is much higher than that in the cool layer. Thus, no obvious decrease of C_2H_2 abundance was found for our sources.

6. Concluding remarks

We analyzed the 14 μm molecular features of 4 optical carbon stars and 4 candidates of infrared carbon stars. The entire spectra of this wavelength region became available thanks to the ISO SWS. It has been revealed that special care should be taken in determining the continuum levels for the analysis of the emission and absorption bands of HCN and C_2H_2 at 14 μm; otherwise the SiC emission at 11 μm as well as molecular absorption at 7.5 μm may lead to the misidentification of spectral features. The main conclusions on the 14 μm molecular bands are as follows;

(1) The emission of HCN $2\nu_2^0$–ν_2^1 bands was detected in the two optical carbon stars, TX Psc and V CrB. This emission feature originates in the circumstellar envelope where HCN molecule in the ground level is pumped to the $2\nu_2^0$ level by 7 μm photon from the photosphere or from the inner envelope.

(2) The broad absorption features due to the C_2H_2 ν_5 bands were detected in the three optical carbon stars, T Lyr, SS Vir and V CrB. These features are basically explained by the absorption in the photosphere or in the warm envelope close to the star.
(3) The absorption of the C_2H_2 ν_5 bands was detected in the 4 infrared sources. This detection finally confirmed the carbon-rich nature of these sources. The absorption features would be formed in the inner envelope in which the mid-infrared radiation originates.

These results give constraints on the modeling of the circumstellar envelope. The higher resolution spectroscopy ($R > 10^4$) will make it possible to distinguish clearly the absorption or emission in the circumstellar envelope from photospheric ones.

Acknowledgements. We are grateful to Dr. K. Noguchi who kindly provided us with the SWS data of the infrared carbon stars. We would like to thank Prof. H. Okuda for taking initiative in our ISO project, and Dr. I. Yamamura for his helpful support in the data reduction. Thanks are also due to Dr. A. Omont for useful comments as a referee especially on infrared carbon stars. W. A. and K. O. acknowledges the Fellowship for young scientists of Japan Society for Promotion of Science.

References

Aoki W., Tsuji T., Ohnaka K., 1998a, A&A 333, L19
Aoki W., Tsuji T., Ohnaka K., 1998b, A&A 340, 222 (Paper I)
Aringer B., Höfner S., Wiedemann G., et al., 1999, A&A 342, 799
Cernicharo J., 1998, Ap&SS 255, 303
Herman M., Huet T.R., Kabbadj Y., Auwera J.V., 1991, Molecular Physics 72, 75
Herzberg G., 1945, Molecular Spectra and Molecular Structure. II., Infrared and Raman Spectra of Polyatomic Molecules. Van Nostrand Reinhold Company, New York
Jørgensen U.G., Hron J., Loidl R., 1999, In: Hron J., Höfner S. (eds.) Abstracts of the 2nd Austrian ISO Workshop, Atmospheres of M, S and C Giants. 51
Justtanont K., Feuchtgruber H., de Jong T., et al., 1998, A&A 330, L17
Kabbadj Y., Herman M., Di Lonardo G., Fusina L., Johns J.W.C., 1991, J. Mol. Spectrosc. 150, 535
Keady J.J., Hinkle K.H., 1988, ApJ 331, 539
Keady J.J., Ridgway S.T., 1993, ApJ 406, 199
Maki A., Quapp W., Klee S., 1995, J. Mol. Spectrosc. 171, 420
Lambert D.L., Gustafsson B., Eriksson K., Hinkle K.H., 1986, ApJS 62, 373
Olofsson H., Eriksson K., Gustafsson B., Carlström U., 1993a, ApJS 87, 267
Olofsson H., Eriksson K., Gustafsson B., Carlström U., 1993b, ApJS 87, 305
Omont A., Loup C., Forveille T., et al., 1993, A&A 267, 515
Ridgway S.T., Carbon D.F., Hall D.N.B., 1978, ApJ 225, 138
Ryde N., Eriksson K., Gustafsson B., 1999, A&A 341, 579
Sloan G.C., Little-Marenin I.R., Price S.D., 1998, AJ 115, 809
Tsuji T., Ohnaka K., Aoki W., Yamamura I., 1997, A&A 320, L1
van der Veen W.E.C.J., Habing H.J., 1988, A&A 194, 125
Weber M., Blass W.E., Halsey G.W., Hillman J.J., 1994, J. Mol. Spectrosc. 165, 107
Wiedemann G.R., Hinkle K.H., Keady J.J., Deming D., Jennings D.E., 1991, ApJ 382, 321
Wirsich J., 1997, Ap&SS 250, 271
Yamamura I., de Jong T., Waters L.B.F.M., Cami J., 1999, In: Le Bertre T., Lébre A., Waelkens C. (eds.) Proc. of IAU Symp. 191, Asymptotic Giant Branch Stars. 267
Yamashita Y., 1972, Ann. Tokyo Astr. Obs. 2nd Ser. 13, 169